P3.8

Nocturnal Stratiform Cloudiness during the West African Monsoon

Jon M. Schrage[1], Stephen Augustyn[1], and Andreas H. Fink[2]

[1]Department of Environmental and Atmospheric Sciences
Creighton University, Omaha, Nebraska

[2]Institute of Geophysics and Meteorology, University of Cologne, D-50923 Cologne, Germany

1. Introduction

Tropical West Africa experiences a summer monsoon circulation that exhibits a number of key features which have been examined to a greater or lesser extent in recent years. Relatively few studies, however, are concerned with the diurnal cycle of the West African monsoon flow or the role of the cloudy zone, often consisting of extensive stratus or stratocumulus cloud decks located south of the main activity belt of mesoscale convective systems as shown in Fig. 1. This region of stratiform cloudiness has been shown to be the zone through which the bulk of the moisture evaporating from the surrounding ocean water is advected inland within the lowest 1-3 km of the atmosphere (Lamb, 1983; Cadet and Nnoli, 1987). The present study attempts to relate striking day-to-day differences in this stratiform cloud regime to large scale changes in the West African monsoon flow and the local boundary layer stability variations.

To achieve this goal, high-resolution vertical profiles of temperature, pressure, and humidity taken from Parakou, Benin during the 2002 NASA IMPETUS project are used, as well as ECMWF (European Center for Medium Range Weather Forecasts) model output. Upon inspection of 00 UTC surface synoptic reports from Parakou, it was found that many nights during the West African monsoon were either completely clear or completely cloudy (7 oktas or more). A dataset of 11 cloudy nights and 12 clear nights between 1 July 2002 and 30 September 2002 was collected, and is presented in Table 1.

2. Composite radiosonde results

The radiosonde observations taken on 11 cloudy nights and 12 clear nights were composited and are shown in Figure 2. While both profiles suggest a moist lower atmosphere, the clear nights (Fig. 2b) were considerably drier than the cloudy nights (Fig. 2a). The clear nights, moreover, exhibited a temperature inversion near the surface that would prevent any buoyant air parcels from rising to their Lifted Condensation Level (LCL) and condensing into low-level clouds. In contrast, a superadiabatic temperature profile near the surface is evident on the cloudy nights, in addition to a well-mixed layer above this region of steep lapse rates. Such a temperature profile would allow for the buoyant production of thermals, and without the presence of a temperature inversion to inhibit convection, these thermals could rise to their LCL and condense, resulting in low-level cloud decks.

Further insight into the structure of the atmosphere on cloudy and clear nights can be gained by comparing profiles of individual variables in their respective soundings, as seen in Figure 3. The African Easterly Jet (AEJ) is quite robust in the zonal wind field on clear nights at about 700 hPa (Fig. 3a), but much less so on cloudy nights, as well as having a more zonal orientation. Below the AEJ, both cloudy and clear nights exhibited weak westerly monsoon flow near the surface, but this flow was stronger on the cloudy nights. At about 150 hPa, which is the level of the Tropical Easterly Jet (TEJ), considerably stronger easterlies were observed on the cloudy nights than on the clear nights. The changes in the zonal wind at all of these levels may reflect different modes of the large scale meteorology of the West African monsoon on these nights.

3. ECMWF results

The differences in the wind fields on cloudy and clear nights evident in the composite radiosonde analyses is also apparent in the composite ECMWF output for the 11 cloudy nights and 12 clear nights of concern. At 00 UTC, the composite 925 hPa streamline chart (Fig. 4c and 4f) illustrates that both clear and cloudy nights exhibit the expected features of the monsoon regime, including cross-equatorial flow, a buffer zone with anticyclonic

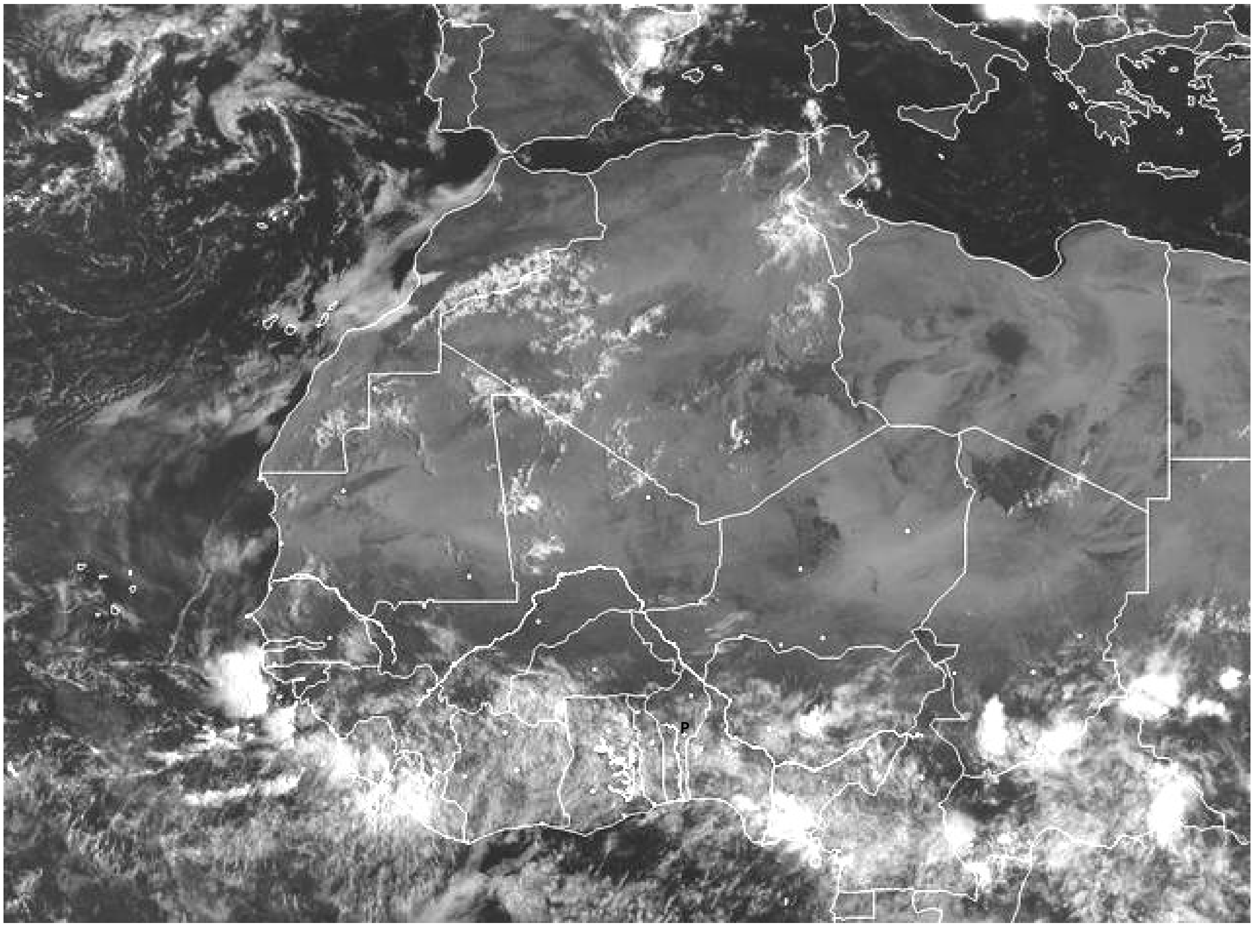

Figure 1: METEOSAT visible satellite image for 09 UTC 22 August 2002, showing much of sub-Sahelian West Africa with stratiform clouds. The location of Parakou is indicated with a “P”.

Table 1:

Cloudy	Clear
4 Jul 2002	5 Jul 2002
10 Jul 2002	8 Jul 2002
17 Jul 2002	11 Jul 2002
30 Jul 2002	20 Jul 2002
1 Aug 2002	27 Jul 2002
2 Aug 2002	3 Aug 2002
6 Aug 2002	10 Aug 2002
7 Aug 2002	28 Aug 2002
22 Aug 2002	3 Sep 2002
27 Aug 2002	8 Sep 2002
30 Sep 2002	17 Sep 2002
	23 Sep 2002

Table 1: Dates of 11 cloudy and 12 clear nights in Parakou, Benin, between 1 July 2002 and 31 September 2002.

curvature, and large scale confluence into the heat low centered near 20° N. This southwesterly onshore flow, however, is considerably stronger on the cloudy nights, which indicates that the strong southwesterly peak at 925 hPa evident in the composite soundings during the cloudy nights at Parkou (Fig. 3a) is embedded in a continental-scale surge of the low-level monsoon westerlies.

The ECMWF results at 700 hPa (Figure 4b and Figure 4e) confirm that the AEJ is more zonal on the clear nights than on the cloudy nights, as well as being more robust. The AEJ is also located farther to the south on clear nights, and the strongest winds were located directly above northern Benin. The cloudy nights, in contrast, featured a trough in the AEJ at approximately 0° W, which may represent a “southern vortex” of an African Easterly Wave (AEW) per the definition of Fink and Reiner (2003).

a. Cloudy Nights:

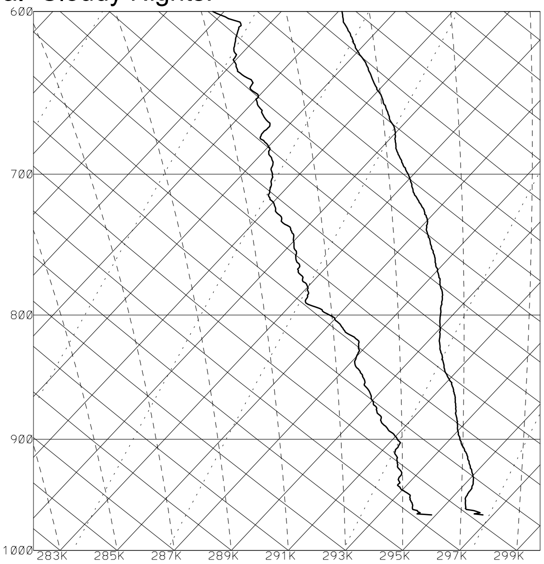

b. Clear Nights:

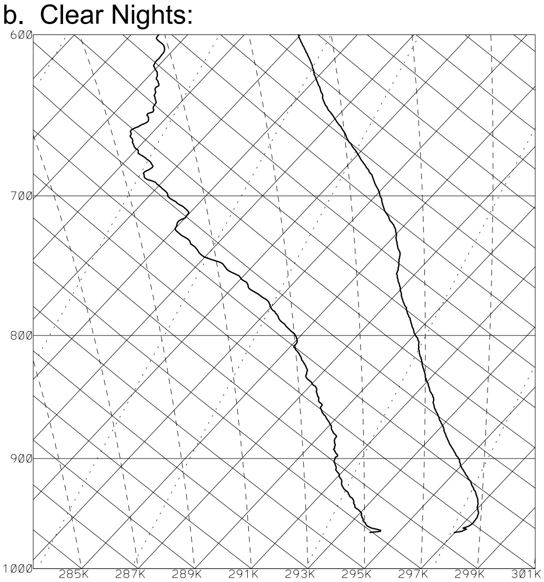

Figure 2: Composite skew *T*-log *P* diagrams of temperature and dewpoint observations below 600 hPa for (a) 11 cloudy nights and 12 (b) clear nights.

Finally, the composite ECMWF results at 200 hPa show that the primary difference between the clear and cloudy nights appears to be in the magnitude of the TEJ. The radiosonde composites exhibited this same relationship, and the correspondence of both the radiosonde composites and the ECMWF composites on the 200 hPa flow lends credence to the possibility that the 700 hPa circulation feature was actually a stationary vortex, as Schrage et al. (2006) described a very strong TEJ during a case of a vortex at 700 hPa during the summer of 2002.

a. b. c.

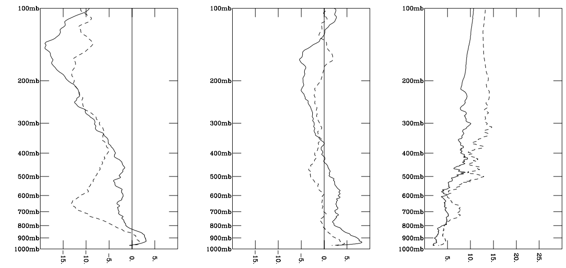

Figure 3: Composite profiles of (a) zonal wind, (b) meridional wind, and (c) dewpoint depression for 11 cloudy nights (solid) and 12 clear nights (dashed).

4. **Moisture**

Composite fields of specific humidity at 925 hPa for the cloudy and clear nights are presented in Fig. 5 using ECMWF operational model data. In both the cloudy and the clear nights, the axis of greatest specific humidity is found to be along approximately 10°N, or approximately the latitudes of the Soudanian climate zone. Steep meridional moisture gradients existed both to the north and the south of this axis, with extremely low specific humidity values north of about 17°N. The chief difference between the moisture fields in the cloudy and clear composites is a moderate reduction in the specific humidity values centered on Benin on the clear nights.

Zonal averages of moisture advection ($-\vec{V}\cdot\nabla q$), moisture divergence ($q\nabla\cdot\vec{V}$), and moisture flux divergence ($\nabla\cdot\left(q\vec{V}\right)$) between 5°W and 5°E at 925 hPa are presented in Fig. 6 for the cloudy and clear nights. Due to the positive meridional gradient of moisture and the southerly flow at 925 hPa, all latitudes south of about 12°N actually experienced *dry air advection* (Fig. 7a) on both the cloudy and the clear nights, with particularly impressive values noted on the cloudy nights along 4°N, where southwesterly flow was especially strong. Conversely, strong moist air advection was noted north of the axis of highest specific humidity, as low level monsoon flow transported moisture towards the heat low over the Sahara. Over most of the West African wet

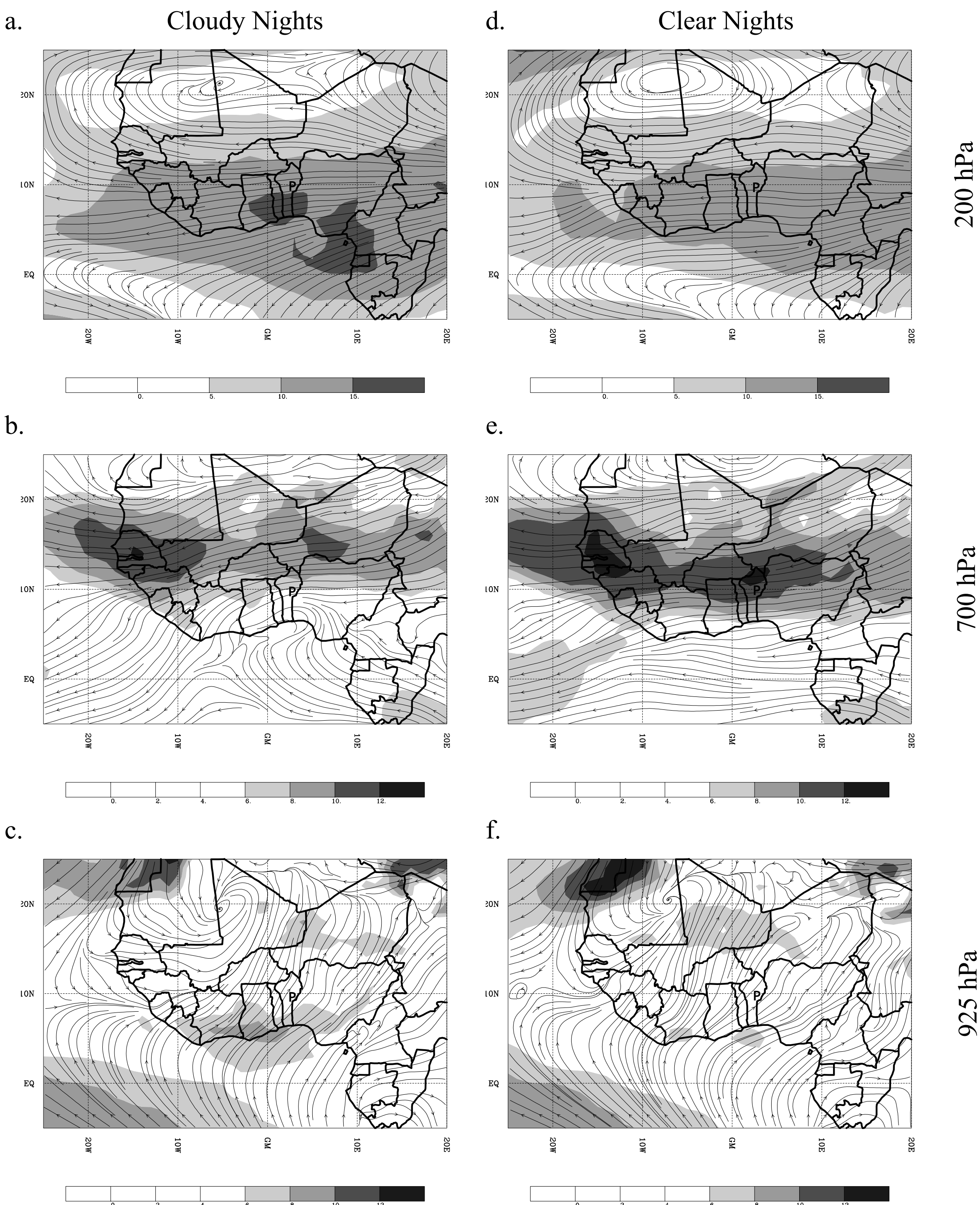

Figure 4: Streamlines and isotachs of the flow at (a) 200, (b) 700, and (c) 925 hPa according to ECMWF operational analyses, composited for 11 cloudy nights. Panels d, e, and f are the same as panels a,b ,c, respectively, except composited for 12 clear nights. Units are m s^{-1}. The location of Parakou is indicated with a “P”.

a. Cloudy Nights:

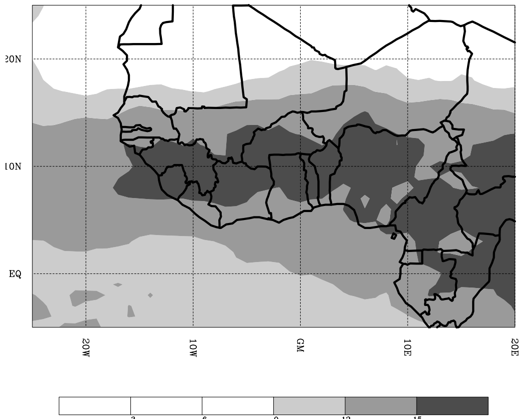

b. Clear Nights:

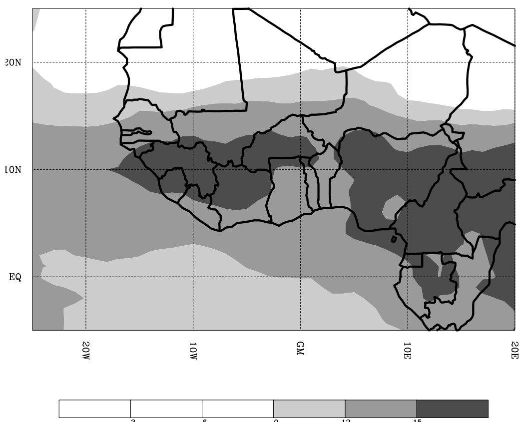

Figure 5. Specific humidity (g/kg) at 925 hPa according to ECMWF operational analyses, composited for (a) 11 cloudy nights and (b) 12 clear nights.

zones, the values of moisture advection are small, negative, and largely independent of the status of the cloud cover; therefore, it seems unlikely that the changes in the low level cloudiness are due to changes in the moisture advection at 925 hPa.

Much greater differences between the cloudy and clear nights are seen in composite fields of moisture divergence at 925 hPa (Fig. 6b). Cloudy nights are characterized by large scale moisture convergence, and upon inspection of the corresponding composite 925 hPa streamlines, it is apparent that this moisture convergence is due to large-scale speed convergence in the boundary layer. In contrast,

a.

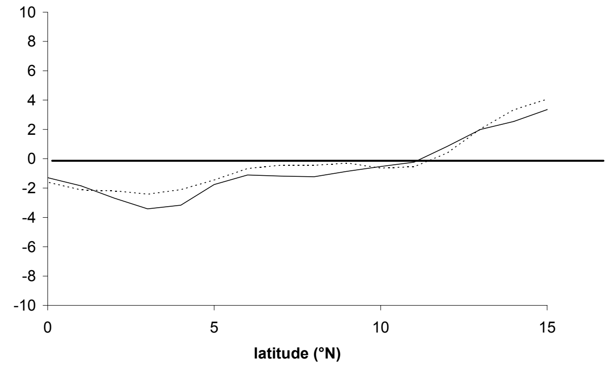

b.

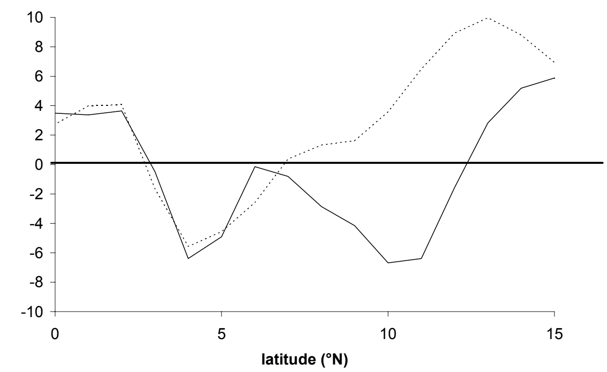

c.

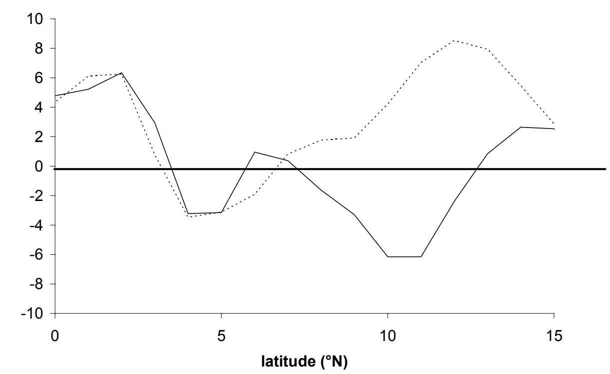

Figure 6: (a) Moisture advection, (b) moisture divergence, and (c) moisture flux divergence in $10^{-8}\ s^{-1}$, zonally averaged between 5°W and 5°E, for cloudy (solid) and clear (dotted) nights.

clear nights exhibited significant moisture divergence at the Sahelian latitudes poleward of 11° N.

On both clear and cloudy nights, the moisture divergence term is considerably larger than the moisture advection term (Fig. 6a and b), and therefore dominates the moisture flux divergence calculation shown in Fig. 6c. As expected, most of sub-Saharan West Africa exhibited a net moisture flux convergence on the cloudy nights, whereas clear nights exhibited slight moisture flux divergence at most latitudes.

It is, therefore, reasonable to infer, based on the composite ECMWF isotach charts at 925 hPa and the moisture divergence calculations, that cloudy nights experience large scale speed convergence in the boundary layer and a positive net moisture flux convergence, whereas clear nights exhibit speed divergence at these levels and moisture flux divergence, at least in the vicinity of Parakou.

5. Low level divergence

In isobaric coordinates, the horizontal momentum equation for the meridional component of the wind can be written as:

$$(1) \qquad \frac{\partial v}{\partial t} + u\frac{\partial v}{\partial x} + v\frac{\partial v}{\partial y} + fu + F_y = -\frac{\partial \Phi}{\partial y}$$

where F_y is the component of friction in the meridional direction and $\Phi = gz$. Assuming steady state conditions, this expression can be rearranged as:

$$(2) \qquad \frac{\partial v}{\partial y} = \underbrace{-\frac{1}{v}\frac{\partial \Phi}{\partial y}}_{A} \quad \underbrace{-f\frac{u}{v}}_{B} \quad \underbrace{-\frac{u}{v}\frac{\partial v}{\partial x}}_{C} \quad \underbrace{-\frac{F_y}{v}}_{D}$$

Therefore, the divergence in the meridional direction (i.e., the left hand side of equation 2) can be explained by four terms, three of which can be computed from the ECMWF operational analyses. Friction (term d) can be calculated as a residual.

Changes in the geopotential height pattern on the 925 hPa surface (not shown) suggested that cloudy nights experience an enhanced meridional pressure gradient poleward of the Soudanian climate zone, suggesting that meridional winds should accelerate northward in this region on those nights, favoring low-level divergence. Fig. 7 supports this conclusion by illustrating that the magnitude of term A from equation 2 is significantly greater on cloudy nights than on clear nights north of approximately 10° N. This contradicts the earlier inference that cloudy nights must have enhanced convergence at 925 hPa (based on the moisture divergence curve shown in Fig. 6b). Therefore, the effects of the enhanced low-level divergence due to changes in the geopotential height pattern must be over-

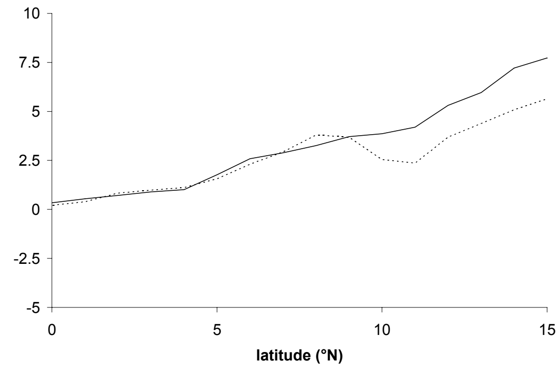

Figure 7. Term A of equation 2, zonally averaged between 5°W and 5°E at 925 hPa, in 10^{-5} s^{-1} for cloudy nights (solid) and clear nights (dashed).

whelmed by convergence driven by another term in equation 2.

Term B was found to be largely invariant between cloudy and clear nights, and term C was found to be small at all latitudes of interest, so it was inferred that term D, the frictional term, made a significant contribution to the low-level convergence that was calculated to be greater on the cloudy nights than on the clear nights. Frictional drag, therefore, may present an important positive feedback for the maintenance of nocturnal stratiform cloud decks during the West African monsoon. Cloudy nights, as shown by the composite radiosonde sounding (Fig. 2a), were capable of persistent production of thermals and maintenance of a well-defined mixed layer due to a superadiabatic lapse rate near the surface. On these nights the boundary layer remains coupled to the surface, and consequently the frictional drag remains high, and winds flowing ashore from the Atlantic Ocean will experience significant speed convergence. This speed convergence results in a net positive moisture flux convergence in the boundary layer, increasing the probability that the rising thermals will result in low cloud production. These stratiform clouds reduce net longwave emission by the surface, helping maintain the instability that kept the boundary layer coupled to the surface. Conversely, on clear nights the coupling of the boundary layer to the surface is greatly diminished by the presence of a strong nocturnal inversion. Winds even a few tens of meters above the surface are largely unaffected by the underlying surface and do not experience substantial frictional drag. Speed convergence is therefore diminished, reducing moisture convergence and making low cloud cover less likely. The reduced cloud cover allows for more radiational cooling of the surface, maintaining the nocturnal inversion that reduced frictional drag. A similar process was described by May (1995) for the nocturnal jet over Australia, in which cloud cover influenced the coupling of the surface to lower level winds.

6. **Summary**

The presence or absence of nocturnal stratiform cloud decks in the wet Soudanian zone during the peak of the West African monsoon season has been found to be a related to a number of key features of the monsoon atmosphere. Clear nights were characterized by the formation of a nocturnal inversion near the surface that decoupled the boundary layer from the surface, therefore reducing the amount of frictional drag and promoting moisture flux divergence, which lowered the moisture content of the lower atmosphere and prevented cloud cover, and the lack of cloud cover permitted further radiational cooling at the surface.

Cloudy nights exhibited a superadiabatic temperature profile near the surface, thus coupling the boundary layer to the surface and allowing for the buoyant production of thermals. Frictional drag was enhanced, as well as speed convergence in the boundary layer due to strong southwesterly monsoon flow, which resulted in a net positive moisture flux convergence. The resulting cloud cover reduced net longwave emission by the surface, therefore helping to maintain the low-level instability evidenced by steep low-level lapse rates.

References

Cadet, B.L., and N.O. Nnoli, 1987: Water vapour transport over Africa and the Atlantic Ocean during summer 1979. *Quart.J.Roy. Meteorol. Soc.,* **113**, 581-602.

Fink, A. H., and A. Reiner, 2003: Spatiotemporal variability of the relation between African Easterly Waves and West African Squall Lines in 1998 and 1999, *J. Geophys. Res.*, 108(D11), 4332, doi:10.1029/2002JD002816.

Lamb, P. J., 1983: West African water vapor variations between recent contrasting Subsaharan rainy seasons. *Tellus*, **35A**, 198-212.

May, P.T., 1995: The Australian nocturnal jet and diurnal variations of boundary-layer winds over Mt. Isa in northeastern Australia. *Quart. J. Roy. Meteor. Soc.*, **121**, 987-1003.

Neelin, J.D. and I.M. Held, 1987: Modeling tropical convergence based on the moist static energy budget. *Mon. Wea. Rev.*, **115**, 3-12.